The Loss Mechanics of Nanoporous Silicon Optical Waveguide for Biochemical Sensors

Susu Yan, Shu-Zee Lo, Paveen Apiratikul, and Professor Thomas E. Murphy

***Abstract*—Nanoporous silicon optical waveguides, which serve as the basic foundation for porous silicon based biochemical sensors, have been fabricated by electrochemical etching and laser local oxidation. By optimizing the porous silicon layers, laser writing power and speed, acceptable optical losses have been achieved. Loss mechanisms include scattering, intrinsic absorption, coupling loss at the fiber interfaces, leakage to the silicon substrate and bending loss. At $1550\,\mathrm{nm}$ wavelength, we report a propagation loss of $10-15\,\mathrm{dB/cm}$, measured using the Fabry Pérot method.**

***Index Terms*—porous silicon, loss mechanism, Fabry Pérot interferometry, biochemical sensors**

I. Introduction

NANOPOROUS silicon is a novel material for optical biochemical sensors due to its large tunable range of refractive indices, and large surface area to volume ratio. Compared with traditional sensors, the large surface area improves the sensitivity of such sensors for detecting small biomolecules. By switching between different current densities in the electrochemical anodization process, porous silicon layers of different porosities can be formed. The refractive indices of such layers are inversely proportional to the porosity, therefore easy to be altered. In a typical optical waveguide, light propagates in core layer with high refractive index surrounded by a low refractive index cladding layer. Such multilayer structures define the vertical confinement of the waveguide. In our project, horizontal confinement is obtained by direct writing through laser local oxidation [1]. Such structures allow biochemical substance detected in the porous silicon core layer by observing changes in optical properties, such as refractive index or absorption coefficient.

Optical waveguide has been used for biosensing for decades. For a slab waveguide structure, substance can be detected by using prism coupler to measure the resonance angle and amplitude changes [2] [3]. To improve the phase sensitivity of the sensors, Mach Zehnder interferometer and other on-chip interference devices need to be fabricated. Molecules can be detected by measuring the phase change between the arm interferometer that is exposed to the molecules and the control arm that is not exposed to the molecules [4]. For this purpose, we need to understand the loss mechanism of porous silicon bent waveguides in order to achieve interferometers.

Optical waveguide losses mainly consist of propagation loss including scattering and intrinsic absorption due to the transmission of light in the guiding layer, coupling loss between lens fibers and cleaved waveguide interfaces, leakage to silicon substrate, and bending loss due to the bent waveguide structure. In this article, we estimate the loss using Fabry Pérot interferometry to be $10-15\,\mathrm{dB/cm}$. We also report optimized parameters for fabricating porous silicon waveguides to minimize the loss.

S. Yan is with Department of Physics, Mount Holyoke College, South Hadley, MA 01075 USA. S.-Z. Lo, P. Apiratikul and T.E. Murphy are with the Department of Electrical and Computer Engineering, University of Maryland, College Park, MD 20742 USA. (e-mail:yan20s@mtholyoke.edu)

II. Waveguide design and Sample Fabrication

A planar waveguide is a slab of dielectric material with high refractive index as a guiding layer surrounded by low refractive index cladding layer. The light only propagates in the slab core layer due to the total internal reflection [5]. A single-mode optical waveguide is needed to ensure further application of on-chip interference devices such as Mach Zehnder, and other phase sensitive devices. For single-mode operation,

$$\frac{\sin\theta_c}{\lambda/2d} \leq 1 \tag{1}$$

must be satisfied, where $\theta_c = \cos^{-1}(\frac{n_1}{n_2})$, n_1 is the core layer refractive index and n_2 is of upper and lower cladding layer, d is the core layer thickness [6]. From Eq. 1, core layer thickness should less than $2.3\ \mu\mathrm{m}$. Based on previous work done in the lab [7], the waveguide is designed of a $1.5\ \mu m$ upper cladding layer, $1.8\,\mu\mathrm{m}$ core layer, and $4.3\,\mu\mathrm{m}$ lower cladding layer, which gave a negligible leakage to the silicon substrate. The relationship between the applied current densities and refractive indices can be found by experimentally measuring the porosities of samples fabricated with different current densities, and subsequently using effective medium approximation or thin film measurement tools such as ellipsoidmetry [8]. This relationship allows easy and flexible fabrication of porous silicon waveguide.

Porous silicon multilayer was fabricated by electrochemical anodization of p-type doped silicon wafer with $10^{20}\ \mathrm{cm}^{-3}$ doping concentration in the HF:Water:Ethanol =1:1:2 solution at room temperature. Upper cladding, core and lower cladding layer are formed by applying current density 210.4, 127.56, and $210.4\ \mathrm{mA/cm}^2$ for 6.1 s, 8.3 s and 17 s which yield thickness of $1.5\ \mu\mathrm{m}$, $1.8\ \mu\mathrm{m}$, and $4.3\ \mu\mathrm{m}$, respectively. The expected porosity was $78\ \%$, $70\ \%$ and $78\ \%$, respectively, which are estimated to be corresponded to refractive index of 1.6, 1.7, and 1.6.

While the multilayer structure with different refractive indices provided the vertical confinement of the optical waveguide, laser local oxidation (Fig. 1) [9] gave the horizontal confinement. A 0.5 hr rapid thermal oxidation procedure at $450°C$ was carried out prior to writing the lines, which partially

oxidized the first few nanometers of the porous silicon surface. Laser beam was emitted by a $473\,\mathrm{nm}$ diode pumped frequency doubled YAG laser, going through a polarization beam splitter to the $40\times(\mathrm{NA}=0.65)$ microscope objective, then focused on the top surface of the porous silicon multilayer. The sample was mounted on the X-Y stage and scanned with different speeds. Oxidized lines were written to be perpendicular to the crystal cleaving lines.

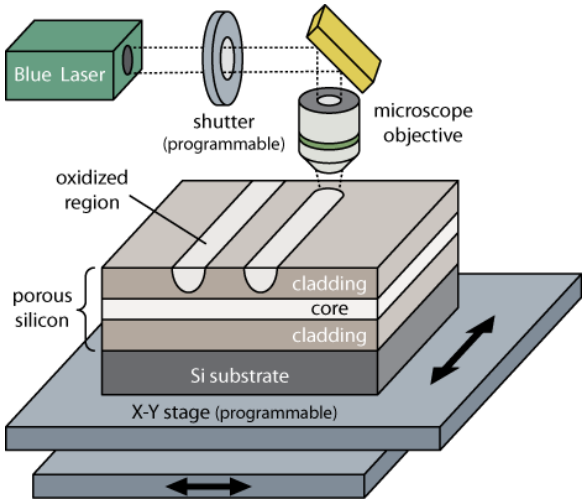

Figure 1. Laser Writing System with $473\,\mathrm{nm}$ blue laser and writing X-Y stage

Then the sample was rinsed in (50% wt.) $\mathrm{HF}:\mathrm{Water}=1:10$ solution etching for $2\,\mathrm{min}$ with gentle agitation to remove the oxidized lines [10]. Followed by a half hour oxidation, light transmission through the waveguide was improved. Finally, the sample was cleaved so that its edge was in perpendicular direction to the waveguide line to reduce coupling loss from lens fiber to the waveguide.

III. Experimental Arrangement and Result

Overall insertion loss was measured using a fiber coupling transmission experiment [11]. Fiber-to-fiber coupling output power at $1550\,\mathrm{nm}$ wavelength was measured to be $0.704\,\mathrm{mW}$. Coupling efficiency was 80%, therefore the input power was $0.879\,\mathrm{mW}$. Coupling to the waveguide was done by adjusting the lens fiber distance to the waveguide edge, centering to the waveguide, and the focusing. For some samples, it was also required to adjust the input polarization. Output power was then measured and optimized with two fibers aligned with the waveguide.

With the goal of optimizing parameters to get low loss porous silicon waveguides, we varied the laser writing speed, power, and waveguide width. Two experimental treatments were accomplished. One was porous silicon optical waveguide written with the same laser power and speed but different waveguide widths aiming to test single-mode or multimode operation. Width was chosen to be 10, 15, 20, and $25\,\mu\mathrm{m}$ from center to center of the two oxidized lines. Single-mode operation was ensured by replacing the output fiber with a $10\times(\mathrm{NA}=0.25)$ microscope objective focused to the output laser beam, and a CCD camera. Single or multi mode operation can be determined by changing the position of the input fiber across the height and the width of the coupling waveguide. Single-mode was demonstrated if the spot only changed in light density but kept the shape in the same position. Most waveguides with $\leq 20\,\mu\mathrm{m}$ width transmit light in a single-mode operation.

In another experiment, we fixed the waveguide width to $20\,\mu\mathrm{m}$ while changing laser power and writing speed to lower the losses. We made several waveguides with combination of laser power of 30, 20, and $10\mathrm{mW}$ and writing speed of 1, 0.5, and $0.25\,\mathrm{mm/s}$ (Fig. 2).

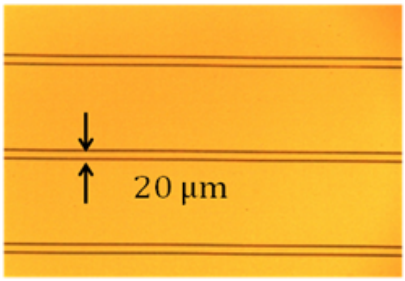

Figure 2. Waveguide fabricated with $30\,\mathrm{mW}$ laser power, $1\,\mathrm{mm/s}$ writing speed

The waveguide fabricated with current density of $210.4\ \mathrm{mA/cm^2}$ for upper and lower cladding layer, $127.56\ \mathrm{mA/cm^2}$ for core layer, local oxidized with $30\,\mathrm{mW}$ laser power, and running X-Y stage at $1\,\mathrm{mm/s}$ speed, had the lowest losses among those tested. Output power of $0.112\,\mathrm{mW}$ was measured with $0.897\,\mathrm{mW}$ of input power. The ratio gave a total insertion loss of $-8.9\,\mathrm{dB}$ including coupling loss, and on-chip propagation loss. The waveguide length was $4.86\,\mathrm{mm}$.

SEM was arranged to have further observation and understanding about optimizing parameters (Fig. 3).

Propagation loss can be estimated by measuring the Fabry Pérot resonance between the two waveguide facets [12]. By varying the wavelength from $1550\,\mathrm{nm}$ to $1551\,\mathrm{nm}$ with $0.001\,\mathrm{nm}$ resolution, we observed Fabry Pérot interference fringes (Fig. 4) from which we calculate the propagation loss [12].

Effective refractive index was estimated by

$$n_{eff}=\frac{\lambda_0^2}{2\Delta\lambda d}$$

where d is the length of the waveguide, and $\triangle\lambda$ is the Fabry Pérot fringe spacing. The n_{eff} of the porous silicon multilayer waveguide was calculated to be 1.6. From Fresnel theory, endfacet reflectivity R given by

$$R=(\frac{n_{eff}-1}{n_{eff}+1})^2=0.047$$

was estimated.

Fringe contrast,

$$K=\frac{T_{max}-T_{min}}{T_{max}+T_{min}}=2.63\times10^{-3}$$

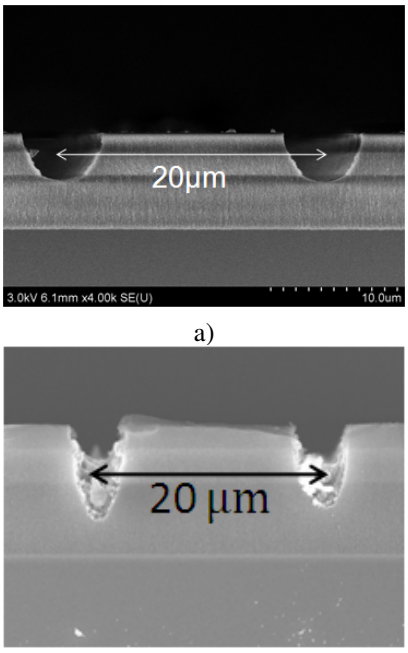

Figure 3. SEM cross-section of porous silicon optical waveguide with a) oxidized line fully removed, b) oxidized line not fully removed

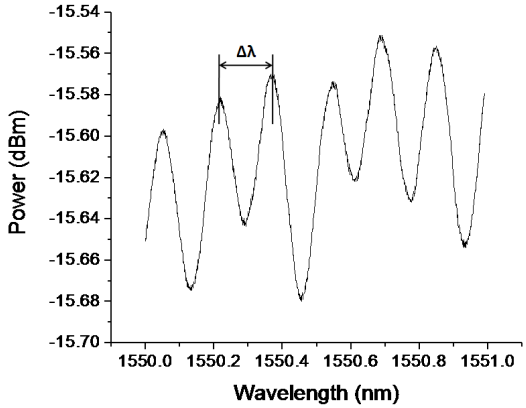

Figure 4. Fabry Pérot interferometry scanning waveguide from 1550 nmto 1551 nm with 0.001 nm resolution

was calculated by averaging all fringe peaks and amplitudes. Since

$$\ln[1 - \frac{(1-K^2)^{1/2}}{K}] = \ln R - \alpha L$$

where L is the waveguide length, and α is propagation loss. Propagation loss was calculated to be $-13\,\mathrm{dB/cm}$. As we discussed above, total loss include propagation loss and coupling loss. Thus by subtracting propagation loss from the total loss, and then dividing by half, coupling loss was calculated to be -2.63 dB.

Beyond straight waveguide, 90° bent waveguide was achieved by moving the X-Y stage in a continuous movement at 1 mm/s speed and under 30mW laser power. Bending radii of 150, 350, 550, and 750 μm were chosen with the same 20 μm wide waveguide (Fig. 5 a). Waveguides were written with the same length to provide same propagation loss with different bending loss. Unfortunately, due to mechanical instability of the writing stages, such losses cannot be measured within the MERIT program period. Mach Zehnder interferometer was fabricated with 550μm radius, 60° bending angle, and 20 μm waveguide width (Fig. 5 b).

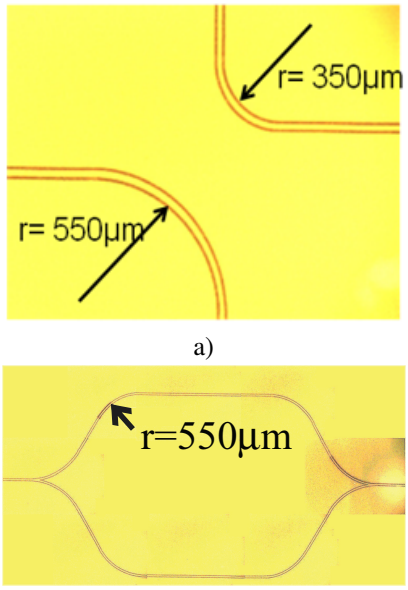

Figure 5. a) Bent waveguides with 350 μm, and 550 μm radius, 20 μm waveguide width b) Mach Zehnder interferometer with 550 μm radius, 60° bending angle, and 20 μm waveguide width

IV. Discussion

Propagation loss, including surface scattering due to the roughness of interfaces of upper cladding-guiding layer, and lower cladding-guiding layer, volume scattering due to the porous silicon structure, and intrinsic absorption to the silicon at guiding layer, was demonstrated to be the main optical loss for nanoporous silicon waveguide. Leakage to the substrate silicon was estimated to be negligible. Moreover, we found scattering loss from the oxidized lines interface act an important role to the on chip propagation loss. As the SEM picture shown, we got -8.9 dB overall insertion loss from the waveguide with oxidized lines been fully removed (Fig. 3 a), but around -33dB loss for other waveguides with oxidized lines not been removed completely (Fig. 3 b). Also, the loss was inversely proportional to the amount of oxidized lines that has been removed. We fabricated six waveguides with same parameters, however, the amount of the lines be removed were different. With less removed oxidized lines, high loss was obtained. Thus, in order to get low loss porous silicon, we demonstrated that the main investigation is to remove the oxidized lines which guarantees a better confinement of the waveguide.

We also demonstrated laser power at 30 mW and writing speed at 1 mm/s, which were both the highest power and speed among all the parameters, gave the lowest loss. The reason is that the oxidized lines were removed under these

parameters. High power and high speed ensure that the porous silicon does not melt when oxidized.

Single-mode operation depends on the vertical and horizontal confinement of the waveguide, which is the thickness of the guiding layer and the width of the waveguide. Determination of the waveguide width is complicated since a gradient of refractive index is formed due to the writing of oxidized lines. On the other hand, reinvestigation of the lines written with $30\,\mathrm{mW}$ and $1\,\mathrm{mm/s}$ was later found to be no longer single mode. The difference between these waveguides and other waveguides written with different parameters suggested that the presence of refractive index gradient in porous silicon waveguide may be due to the stress associated with the lattice mismatch between oxidized lines and porous silicon. Once the oxidized lines are completely removed, such stress was also removed, thus the removal of refractive index gradient.

Polarization dependence of porous silicon waveguide are also required further investigation. While there was polarization dependent loss in waveguide with partial oxidized lines, the waveguide with oxidized lines completely removed showed no polarization dependent loss.

V. Conclusions

We have studied the basic loss mechanisms of nanoporous silicon optical waveguide. We demonstrated the propagation loss is the main loss contributing to the overall insertion loss for porous silicon optical waveguide. Low loss waveguide has been fabricated, and Fabry Pérot interferometry was used to measure the loss. Optimized parameters to achieve low loss waveguide have been found, and can be used for further waveguide study, biochemical sensors fabrication, and other on chip interference devices. Based on our project, we believe the ultimate goal to achieve low loss porous silicon optical waveguide is to completely remove the oxidized lines. Polarization characteristics need further testing. Complex waveguide pattern, such as bent waveguide with different radius and different travel angles, and Mach Zehnder interferometer were achieved, although measurements cannot be completed due to mechanical instability in the writing stages. In order to know more details about the optical losses mechanism, further study about the contribution of scattering and intrinsic absorption need to be investigated.

References

[1] A. M. Rossi, G. Amato, V. Camarchia, L. Boarino, and S. Borini, "High-quality porous-silicon buried waveguide," *Appl. Phys. Lett.*, vol. 78, p. 20, 2001.

[2] G. Rong, A. Najmaie, J. E. Sipe, and S. M. Weiss, "Nanoscale porous silicon waveguide for label-free dna sensing," *Biosens. Bioelectron.*, vol. 23, p. 1572, 2008.

[3] A. M. Rossi, L. Wang, V. Reipa, and T. E. Murphy, "Porous silicon biosensor for detection of viruses," *Biosensors and Bioelectronics*, vol. 23, pp. 741–745, 2007.

[4] S. Weiss, G. Rong, and J. Lawrie, "Current status and outlook for silicon-based optical biosensors," *Physica*, vol. E 41, pp. 1071–1075, 2009.

[5] G. Rong, J. D. Ryckman, R. L. Mernaugh, and S. M. Weiss, "Label-free porous silicon membrane waveguide for dna sensing," *Appl. Phys. Lett.*, vol. 93, p. 161109, 2008.

[6] B. E. A. Saleh and M. C. Teich, *Fundamentals of Photonics*. Wiley Interscience Publication, 1991.

[7] P. Apiratikul, A. M. Rossi, and T. E. Murphy, "Nonlinearities in porous silicon optical waveguides at 1550 nm," *Opt. Express*, vol. 17, pp. 3396–3406, 2009.

[8] D. E. Aspnes and J. B. Theeten, "Investigation of effective -medium models of microscopic surface roughtness by spectroscopic ellipsometry," *Phys. Rev. B*, vol. 20, pp. 3292–3302, 1979.

[9] I. Rea, A. Marino, M. Iodice, G. Coppola, I. Rendina, and L. D. Stefano, "A porous silicon bragg grating waveguide by direct laser writing," *J. Phys.: Condens. Matter*, vol. 20, p. 365203, 2008.

[10] L. D. Stefano, I. Rea, M. A. Nigro, F. G. D. Gorte, and I. Rendina, "A parametric study of laser induced ablationŰoxidation on porous silicon surfaces," *J. Phys.: Condens. Matter*, vol. 20, p. 265009, 2008.

[11] A. Loni, L. Canham, M. Berger, R. Arens-Fischer, H. Munder, H. Luth, H. Arrand, and T. Benson, "Porous silicon multilayer optical waveguides," *Thin Solid Films*, vol. 276, pp. 143–146, 1996.

[12] R. Deri and E. Kapon, "Low-loss iii-v semiconductor optical waveguides," *IEEE J. Quantum Electron.*, vol. 27, pp. 626–640, 1991.